Geochimica et Cosmochimica Acta Vol. 56, pp. 1545–1560

0016-7037/92/$5.00 + .00

Organic sulphur in macromolecular sedimentary organic matter. II. Analysis of distributions of sulphur-containing pyrolysis products using multivariate techniques*

TIMOTHY I. EGLINTON,[†‡] JAAP S. SINNINGHE DAMSTÉ,[1] WIM POOL,[1] JAN W. DE LEEUW,[1]
GERT EIJKEL,[2] and JAAP J. BOON[2]

[1]Organic Geochemistry Unit, Faculty of Chemical Engineering and Materials Science, Delft University of Technology, De Vries van Heystplantsoen 2, 2628RZ Delft, The Netherlands
[2]FOM Institute for Atomic and Molecular Physics, Kruislaan 407, 1098SJ Amsterdam, The Netherlands

(*Received September* 28, 1990; *accepted in revised form January* 14, 1992)

Abstract—This study describes the analysis of sulphur-containing products from Curie-point pyrolysis (Py) of eighty-five samples (kerogens, bitumen, and petroleum asphaltenes and coals) using gas chromatography (GC) in combination with sulphur-selective detection. Peak areas of approximately forty individual organic sulphur pyrolysis products (OSPP) were measured, and the results analysed with the aid of multivariate data reduction techniques (principal components analysis, (PCA)). The structural relationships proposed in an earlier publication (SINNINGHE DAMSTÉ et al., 1989a) in which OSPP can be grouped according to common "carbon skeletons" are supported by PCA. The distribution of OSPP varies both as a function of kerogen type (as defined by elemental composition) and maturity, reflecting differences in the relative abundance of the various carbon skeleton types. Sulphur-containing products from Type I, Type II, and, to some extent, Type II-S kerogens are dominated by OSPP derived from "moieties" (i.e., discrete structural components within the macromolecule) possessing linear carbon skeletons, while coals and Type III kerogens give rise to higher relative abundances of OSPP with branched carbon skeletons. Type I kerogens are distinguished from Type II kerogens due to the type of linear carbon skeleton, the former yielding higher relative amounts of 2-*n*-alkylthiophenes and thiolanes and the latter 2,5-di-substituted sulphur-containing products. Products from sulphur-rich (Type II-S) kerogens differ by higher relative abundances of OSPP derived from precursors with isoprenoid and/or steroidal side-chain carbon skeletons, and by higher absolute abundances of all OSPP.

Petroleum and, to a lesser extent, bitumen asphaltenes give rise to OSPP with longer carbon skeletons than do kerogens or coals. This observation supports the models proposed by SINNINGHE DAMSTÉ et al. (1990a) in which sulphur-containing moieties in asphaltenes are bound by fewer intermolecular bridges (i.e., are less extensively cross-linked) and, consequently, more readily yield longer chain products on pyrolysis.

From these observations, we suggest that Py-GC in combination with PCA provides useful information concerning the chemical nature of organically bound sulphur in geomacromolecules. This information can be rationalised based on carbon skeleton relationships established for low molecular weight organic sulphur compounds, and in terms of kerogen type and overall sulphur content.

INTRODUCTION

THE ANALYSIS of organic sulphur in sedimentary organic matter has now become an integral part of organic geochemistry (ORR and WHITE, 1990; SINNINGHE DAMSTÉ, 1988; DE LEEUW and SINNINGHE DAMSTÉ, 1990). Much progress has been made in the identification of organic sulphur compounds in sediment extracts and in determining their relationship to biological precursor molecules (e.g., BRASSELL et al., 1986; SINNINGHE DAMSTÉ et al., 1988b; 1989b,d). The nature of organically bound sulphur in macromolecular organic matter (e.g., kerogens, coals, and asphaltenes) is presently less well understood. There is, however, strong evidence that under the appropriate conditions (i.e., prevalent sulphate reduction, low reactive iron availability, and a high content of labile organic carbon), sulphur may be introduced into and indeed promote the formation of, non-GC amenable higher molecular weight organic substances through similar mechanisms to those postulated for individual molecules. The latter are believed to arise through incorporation of inorganic sulphur species (H_2S, polysulphides) into functionalised lipids during the early stages of diagenesis (SINNINGHE DAMSTÉ et al., 1988b; 1989b; 1990a; TEGELAAR et al., 1989). The sulphur-containing components of low- and high-molecular-weight organic fractions (asphaltenes and kerogens) are therefore perceived to be comprised of similar subunits. The main difference is believed to lie in the degree of intermolecular sulphur cross-linking in low- vs. high-molecular-weight sedimentary organic substances (SINNINGHE DAMSTÉ et al., 1990a; KOHNEN et al., 1991).

Flash pyrolysis represents one method of providing direct information concerning the chemical nature of macromolecularly bound sulphur (BOUDOU et al., 1987; EGLINTON et al., 1988; 1990a,b; PHILP et al., 1988; SINNINGHE DAMSTÉ et al., 1988a; 1989a; 1990a). The major OSPP of sulphur-rich ($S_{org}/C > 0.04$, e.g., Miocene Monterey Formation)

* For parts I, III and IV see SINNINGHE DAMSTÉ et al. (1989a), EGLINTON et al. (1990a,b), respectively.

† To whom correspondence should be addressed.
‡ *Present address:* Dept. of Chemistry, Woods Hole Oceanographic Institution, Woods Hole, MA 02543, USA.

kerogens have been found to be C_4–C_{10} compounds of which thiophenes are generally by far the most dominant compound class (SINNINGHE DAMSTÉ et al., 1988a; 1989a). Alkylthiolanes, alkenylthiophenes, and alkylbenzothiophenes have also been identified in flash pyrolysates of these materials (SINNINGHE DAMSTÉ et al., 1988a). These OSPP have been shown to be directly derived from the macromolecular matrix and not artefacts (i.e., secondary products) of the pyrolysis procedure (EGLINTON et al., 1990a). With respect to the C_4–C_{10} thiophenes, the major mechanisms of formation upon pyrolysis are believed to be either cleavage of C-C bonds in alkyl sidechains β- to the thiophene ring, or scission of relatively weak S-S and C-S bridges within and between molecules (SINNINGHE DAMSTÉ et al., 1990a). It has been noted that the abundance (both relative to hydrocarbons and in absolute amounts) and distribution of OSPP varies both with kerogen type (EGLINTON et al., 1990a) and maturity (EGLINTON et al., 1988; 1990b). It has also been observed that sulphur-containing moieties (i.e., structurally discrete subunits) in kerogens and asphaltenes give rise to OSPP with similar structures to those commonly observed in the GC-amenable fractions of diagenetically immature sulphur-rich sediment extracts and oils (SINNINGHE DAMSTÉ et al., 1989a). The compositional similarities between sulphur-containing compounds associated with these different organic fractions lend support to the view that the OSPP are derived from common structural units. The similarity between isomer (carbon skeleton) distributions of sulphur compounds in pyrolysates of kerogens corresponding asphaltenes and low molecular weight organic sulphur compounds in the bitumen for a given source rock also suggests a genetic link between the low molecular weight and high molecular weight fractions of sedimentary organic matter (SINNINGHE DAMSTÉ et al., 1989a; 1990a). OSPP distributions have also been found to reflect the bulk carbon skeleton content of the kerogen (DOUGLAS et al., 1991; DERENNE et al., 1990). Consequently, it has been proposed that the major OSPP may be attributed to one or more of the following four precursor carbon skeletons: linear; branched; isoprenoid; and steroid (SINNINGHE DAMSTÉ et al., 1989a). These relationships are summarized in Fig. 1.

The above observations have led us to examine the distributions of OSPP from a wide variety of samples differing in both organic matter type and thermal maturity. The present study describes the analysis of eighty-five samples (kerogens, coals, oil, and bitumen asphaltenes) by Py-GC using a sulphur-selective flame photometric detector (FPD). Integrated peak areas of approximately forty compounds were determined. The large number of OSPP quantified together with the size of the sample set necessitated that data reduction be implemented. Multivariate analysis using PCA was chosen since this technique has previously been successfully applied to Py-GC data (e.g., ØYGARD et al., 1988; RYAN-GRAY et al., 1991) but has not previously been used to study distributions of sulphur-containing products. The Py-GC–FPD data were analysed using PCA in order to reveal the major features of the OSPP distributions which distinguish samples either as a function of organic matter type or maturity. It was anticipated that PCA would be particularly useful for the present study in the following two ways: (1) to provide an objective assessment of the carbon skeleton relationships proposed earlier (SINNINGHE DAMSTÉ et al., 1989a); and (2) to determine the extent and type of geochemical information which might be available through analysis of macromolecularly bound sulphur using this approach.

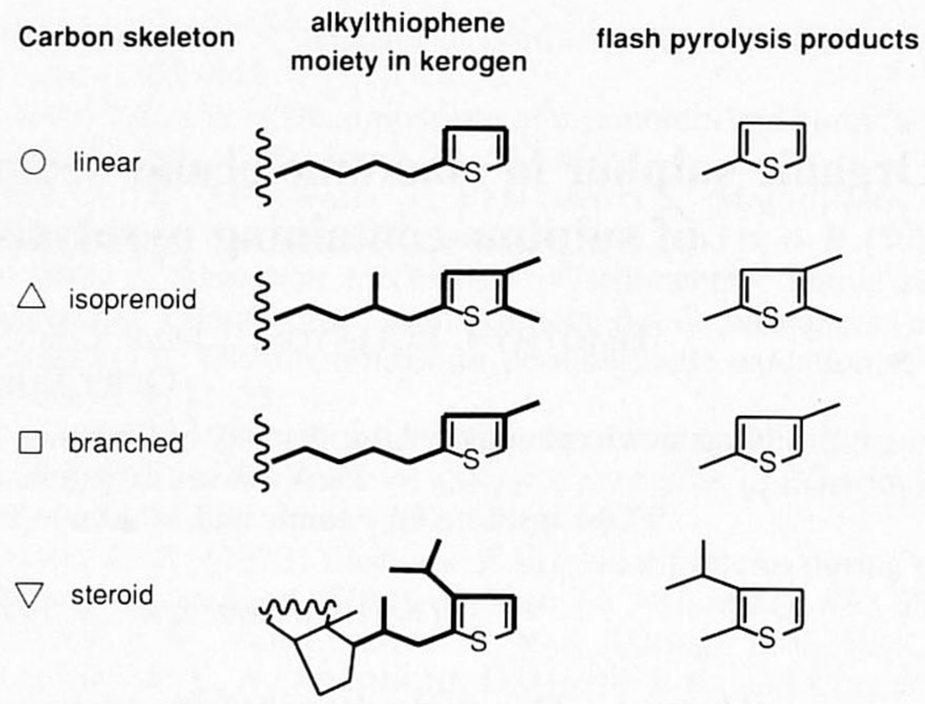

FIG. 1. Proposed structural relationships between alkylthiophene moieties in kerogens and asphaltenes and their presumed flash pyrolysis products (modified after SINNINGHE DAMSTÉ et al., 1989a). Examples are given for alkylthiophene moieties with linear, isoprenoid, branched, and steroidal side-chain carbon skeletons. Carbon skeletons are indicated with bold lines.

EXPERIMENTAL

The samples analysed for this study are listed in Table 1 together with selected geochemical data. "Kerogen Type" was assigned primarily based on elemental analysis (when available) or Py-GC data. Asphaltenes generally have higher H/C and lower O/C and S/C ratios than do kerogens and hence do not strictly follow the same classification. Bitumen asphaltenes were therefore ascribed according to corresponding kerogen composition. In the case of petroleum asphaltenes, assignments were made based on literature data describing the compositions of the inferred immature source rock kerogen.

Rock samples were either soxhlet or ultrasonically extracted using dichloromethane and methanol and demineralised according to previously published HF/HCl digestion procedures (EGLINTON et al., 1988) in order to isolate kerogens. Asphaltenes were precipitated at room temperature from oils and solvent extracts using an excess of *n*-hexane or *n*-heptane. Py-GC conditions have been described in detail previously (SINNINGHE DAMSTÉ et al., 1988a; 1989a). Briefly, a Curie-point pyrolysis system (Curie Temp., 610°C; 10 sec, pyrolysis time) was directly interfaced to a gas chromatograph equipped with both a flame ionization detector (FID) and a FPD. The pyrolysis products were separated on a fused silica capillary column coated with an apolar stationary phase (CP Sil-5, Chrompak), and the effluent was split to both detectors. Peak assignments were made on the basis of coelution with authentic standards, retention indices, and selected Py-GC–MS analyses (SINNINGHE DAMSTÉ et al., 1988a). Integrated peak areas from the FPD chromatograms were obtained using "Maxima" (Waters Assoc.) chromatography software. The square root of each peak area was calculated to compensate for the quadratic response of the FPD (FARWELL and BARINAGA, 1986) which would otherwise excessively influence variance in the data set. These data were subjected to PCA using the FOM-PYRODAT package for multivariate analysis of Py-MS and Py-GC data. This package employs parts of an early version of the ARTHUR programme released by Infometrix (Seattle, WA, U.S.A., 1977 version) and utilises a VAX 11/785 computer system. The data were introduced via an IBM-type personal computer using Lotus 1-2-3 software. The principles of the ARTHUR-based PCA are described by WINDIG et al. (1982). Results from this procedure are output as loadings (variables) and scores (samples). Studies using the same approach and describing

TABLE 1. GENERAL AND GEOCHEMICAL DESCRIPTIONS OF SAMPLES

Sample Location and depth	Form[a]	Code	Age	TOC(%)	Ro(%)[b]	Tmax(C)[c]	HI[c]	H/C[d]	S/C[d]	Sorg/C[d]	[TR][e]	Type[f]
Aleksinac shale, Jugoslavia	K	Al	Olig.	n.d.	n.d.	n.d.	n.d.	n.d.	n.d.	n.d.	n.d.	I
Athabasca Tar Sand, Canada	O	At	Cret.	n.a.	n.a.	n.a.	n.a.	n.d.	n.d.	n.d.	0.23	II
Autun shale, Surmoulin, France	K	Au	Perm.	12.6	0.40	432	318	1.08	0.005	n.d.	0.09	II
Bark coal, China	C	Bk	Eoce.	52.8	0.57	452	362	n.d.	n.d.	n.d.	0.11	III
Brown Lst., Gulf of Suez 957m	K	B1	Cret.	4.7	n.d.	412	438	1.55	0.140	0.106	0.64	II-S
Brown Lst., Gulf of Suez 1521m	K	B2	Cret.	4.7	n.d.	402	406	1.71	0.100	0.076	0.70	II-S
Cameroon, Africa 1752m	K	Ca	Cret.	n.d.	n.d.	n.d.	n.d.	1.19	0.039	n.d.	0.26	II
Cherokee coal, IA, USA	C	Ch	Cret.	53.9	0.38	423	194	0.85	0.041	0.041	0.39	III
Gardanne coal, France	C	Ga	?	74.2	0.48	424	181	0.81	0.031	n.d.	0.49	III
Green River shale, CO, USA	K	Gr	Eoce.	7.9	0.31	444	777	1.54	0.029	n.d.	0.09	I
Guttenberg shale, WI, USA	K	Gu	Ordo.	8.0	n.d.	440	919	1.49	0.025	0.007	0.04	I
Mahakam coal, Indonesia 1390m	C	I1	Tert.	66.2	0.38	420	275	0.95	0.012	0.007	0.15	III
Mahakam coal, Indonesia 1920m	C	I2	Tert.	69.1	0.43	424	278	0.94	0.011	0.008	0.15	III
Mahakam coal, Indonesia 2020m	C	I3	Tert.	71.1	0.47	420	291	0.94	0.011	0.008	0.13	III
Mahakam coal, Indonesia 2480m	C	I4	Tert.	74.3	0.52	435	274	0.95	0.007	0.005	0.07	III
Illinois #6 coal, IL, USA	C	IL	?	79.6	0.47	421	168	0.76	0.021	0.013	0.34	III
Jurf ed Darawish shale, Jordan 45m	K	J1	Cret.	5.1	0.25	409	774	1.42	0.079	n.d.	0.88	II-S
Jurf ed Darawish shale, Jordan 45m	B	J2	Cret.	n.a.	n.a.	n.a.	n.a.	1.40	0.052	0.052	0.71	II-S
Jurf ed Darawish shale, Jordan 100m	K	J3	Cret.	7.1	0.28	407	820	1.38	0.086	n.d.	0.76	II-S
Jurf ed Darawish shale, Jordan 100m	B	J4	Cret.	n.a.	n.a.	n.a.	n.a.	1.51	0.073	0.073	1.10	II-S
Jurf ed Darawish shale, Jordan 156m	K	J5	Cret.	16.8	0.30	416	892	1.60	0.084	n.d.	0.80	II-S
Jurf ed Darawish shale, Jordan 156m	B	J6	Cret.	n.a	n.a	n.a	n.a.	1.44	0.072	0.072	1.16	II-S
Jet Rock, Yorks., UK	K	Jt	Lias	7.9	0.37	435	613	1.40	0.220	n.d.	0.16	II
Kimmeridge shale, Dorset, UK	K	K1	U.Jur.	45.7	0.35	421	589	1.24	0.055	0.047	0.56	II/II-S
Kimmeridge shale, Dorset, UK	B	K2	U.Jur.	n.a.	n.a.	n.a.	n.a.	1.23	0.032	0.032	0.57	II
Kimmeridge shale, Dorset, UK	K	K3	U.Jur.	45.7	0.35	421	589	1.24	0.055	0.047	0.56	II/II-S
Kimmeridge shale, Yorks., UK	K	K4	U.Jur.	4.6	0.44	416	408	1.22	0.019	0.017	0.33	II
Kimmeridge shale, Yorks., UK	K	K5	U.Jur.	24.3	0.47	419	219	1.32	0.029	0.008	0.34	II
Kimmeridge shale, North Sea 2065m	K	K6	U.Jur.	n.d.	0.40	n.d.	n.d.	1.25	n.d.	n.d.	0.30	II
Kimmeridge shale, North Sea	K	K7	U.Jur.	n.d.	n.d.	n.d.	n.d.	n.d.	n.d.	n.d.	n.d.	II
Kimmeridge HY-PY, Dorset, UK	K	K8	U.Jur.	n.d.	0.95	n.d.	n.d.	1.00	0.083	n.d.	0.28	II
La Luna shale, Venezuela	K	LL	Cret.	10.0	0.55	432	513	n.d.	n.d.	n.d.	0.27	II
Marl Slate, North Sea	K	Ma	Perm.	9.2	0.45	423	339	1.13	0.072	n.d.	0.27	II
Messel shale, FRG	K	Me	Eoce.	26.8	0.27	430	436	1.37	0.011	n.d.	0.03	I/II
Monterey shale, CA, USA	K	M1	Mioc.	18.6	0.15	393	555	1.33	n.d.	0.070	1.81	II-S
Monterey shale, CA, USA	K	M2	Mioc.	23.7	0.39	400	484	1.45	0.058	n.d.	1.12	II-S
Monterey shale, CA, USA	K	M3	Mioc.	13.0	0.46	403	479	n.d.	n.d.	n.d.	1.01	II-S
Monterey shale, CA, USA	B	M4	Mioc.	n.a.	n.a.	n.a.	n.a.	1.44	0.044	0.044	1.09	II-S
Monterey shale, CA, USA	K	M5(3)	Mioc.	17.3	0.33	401	352	1.28	0.061	0.054	0.82	II-S
Monterey shale, CA, USA	K	M6(2)	Mioc.	n.d.	n.d.	n.d.	n.d.	n.d.	n.d.	n.d.	1.48	II-S
Monterey shale, CA, USA 1326m	K	M7	Mioc.	3.8	n.d.	393	458	1.32	0.137	0.070	1.59	II-S
Monterey shale, CA, USA 2362m	K	M8	Mioc.	6.5	n.d.	389	553	1.17	0.144	0.060	1.38	II-S
Monterey shale, CA, USA 3651m	K	M9	Mioc.	3.6	n.d.	418	503	1.21	0.353	0.102	0.64	II-S
Monterey shale, CA, USA 4063m	K	M10	Mioc.	3.5	n.d.	421	411	1.09	0.156	0.048	0.54	II-S
Monterey shale, CA, USA	O	M11	Mioc.	n.a.	n.a.	n.a.	n.a.	1.37	0.042	0.042	0.59	II-S
Monterey shale, CA, USA	O	M12	Mioc.	n.a.	n.a.	n.a.	n.a.	1.21	0.025	0.025	0.42	II-S
Monterey shale, CA, USA	O	M13	Mioc.	n.a.	n.a.	n.a.	n.a.	n.d.	n.d.	n.d.	n.d.	II-S
New Albany shale, IN, USA	K	Ne(2)	Devo.	21.9	0.47	429	349	1.05	0.047	0.014	0.09	II
Oulad Abdoun shale, Morocco	K	O1	Maas.	14.5	0.40	394	822	1.33	0.085	0.081	1.02	II-S
Oulad Abdoun shale, Morocco	K	O2	Maas.	1.1	n.d.	416	237	1.06	0.074	0.073	1.02	II-S
Oulad Abdoun shale, Morocco	K	O3	Maas.	3.2	n.d.	n.d.	n.d.	1.02	0.071	0.068	0.64	II-S
Oulad Abdoun shale, Morocco	K	O4	Maas.	1.7	n.d.	392	456	1.32	0.079	0.075	1.15	II-S
Oulad Abdoun shale, Morocco	K	O5	Maas.	2.8	0.41	416	682	n.d.	n.d.	n.d.	1.08	II-S
Paris Basin, France 9m	K	P1	Toar.	8.0	0.33	424	523	n.d.	n.d.	n.d.	0.30	II
Paris Basin, France 22m	K	P2	Toar.	8.1	0.37	424	736	n.d.	n.d.	n.d.	0.26	II
Paris Basin, France 30m	K	P3	Toar.	5.8	0.41	426	601	n.d.	n.d.	n.d.	0.19	II
Paris Basin, France 30m	K	P4	Toar.	6.5	0.32	427	672	n.d.	n.d.	n.d.	0.23	II
Paris Basin, France 1016m	K	P5	Toar.	7.1	0.36	427	692	n.d.	n.d.	n.d.	0.26	II
Paris Basin, France 1320m	K	P6	Toar.	7.2	0.36	425	662	n.d.	n.d.	n.d.	0.28	II
Paris Basin, France 2008m	K	P7	Toar.	2.9	0.43	436	536	n.d.	n.d.	n.d.	0.27	II
Paris Basin, France 2430m	K	P8	Toar.	7.9	0.42	440	598	n.d.	n.d.	n.d.	0.24	II
Phosphoria shale, MO, USA	K	Ph(2)	Perm.	15.3	0.28	423	643	1.43	0.068	n.d.	0.83	II-S
Posidonia shale, FRG	K	Po	Toar.	3.0	0.38	429	424	1.64	0.051	n.d.	0.20	II
Pittsburg coal, PA, USA	C	Pt	Penn.	81.3	0.65	430	282	0.79	0.023	0.009	0.09	III
Rozel Point oil, UT, USA	O	R1	Mioc.	n.a.	n.a.	n.a.	n.a.	1.53	0.074	0.074	0.43	II-S
Rozel Point seep oil, UT, USA	O	R2	Mioc.	n.a.	n.a.	n.a.	n.a.	n.d.	n.d.	n.d.	0.56	II-S
Rasa Lignite, Yugoslavia	C	Rs	Tert.	73.8	0.68	n.d.	n.d.	0.78	0.055	0.053	0.47	III-S
Sarsina, Italy	B	Sa	Mioc.	n.a.	n.a.	n.a.	n.a.	1.52	0.056	0.056	0.70	II-S
Serpiano shale, Switzerland	K	S1	Tria.	33.1	0.37	416	762	1.27	0.057	n.d.	0.63	II/II-S
Serpiano shale, Switzerland	K	S2	Tria.	30.8	n.d.	407	535	n.d.	n.d.	n.d.	0.65	II-S
SMB, Southampton I., Canada	K	Si	?	21.4	n.d.	423	561	n.d.	n.d.	n.d.	0.27	II
Tarfaya shale, Morocco	K	Tf	Maas.	n.d.	n.d.	n.d.	n.d.	n.d.	n.d.	n.d.	0.61	II-S
Tasmanite, Australia	K	Tm	Perm.	28.8	n.d.	444	912	1.48	0.004	n.d.	0.08	I/II
Timahdit shale, Morocco	K	T1	Maas.	3.9	0.38	n.d.	n.d.	1.36	0.061	0.056	0.86	II-S
Timahdit shale, Morocco	K	T2	Maas.	14.2	n.d.	n.d.	n.d.	1.39	0.075	0.063	0.86	II-S
Timahdit shale, Morocco	K	T3	Maas.	n.d.	n.d.	n.d.	n.d.	1.42	0.060	n.d.	0.62	II-S
Vinini shale, NE, USA	K	Vi	Ordo.	21.3	n.d.	434	551	1.21	0.026	n.d.	0.22	I/II
Woodford shale, OK, USA	K	Wd	Devo.	16.2	n.d.	438	442	1.16	0.029	n.d.	0.27	II
Womble shale, OK, USA	K	Wo	Ordo.	14.6	n.d.	428	405	1.13	0.036	n.d.	0.24	II
Westfield shale, Scotland	K	Wf	Carb.	34.8	0.41	444	650	1.27	0.007	n.d.	0.01	I

[a]Form: K = kerogen; C = coal; O = oil asphaltene; B = bitumen asphaltene.
[b]Ro(%): Vitrinite reflectance (in oil).
[c]Tmax (°C) and Hydrogen Index (HI) determined from temperature-programmed "Rock-Eval" pyrolysis of whole rock samples.
[d]Atomic ratios determined from elemental analysis of isolated kerogens or asphaltenes.
Sorg. determined by correction for Fe (pyrite) content.
[e][TR]: [2,3-dimethylthiophene]/[1,2-dimethylbenzene + *n*-non-1-ene] (Eglinton *et al.*, 1990a).
[f]Type: Inferred kerogen type based on elemental $S_{org.}$/C and TR (when available) or inferred from OSPP distributions (this study).
n.d. = not determined; n.a. not applicable

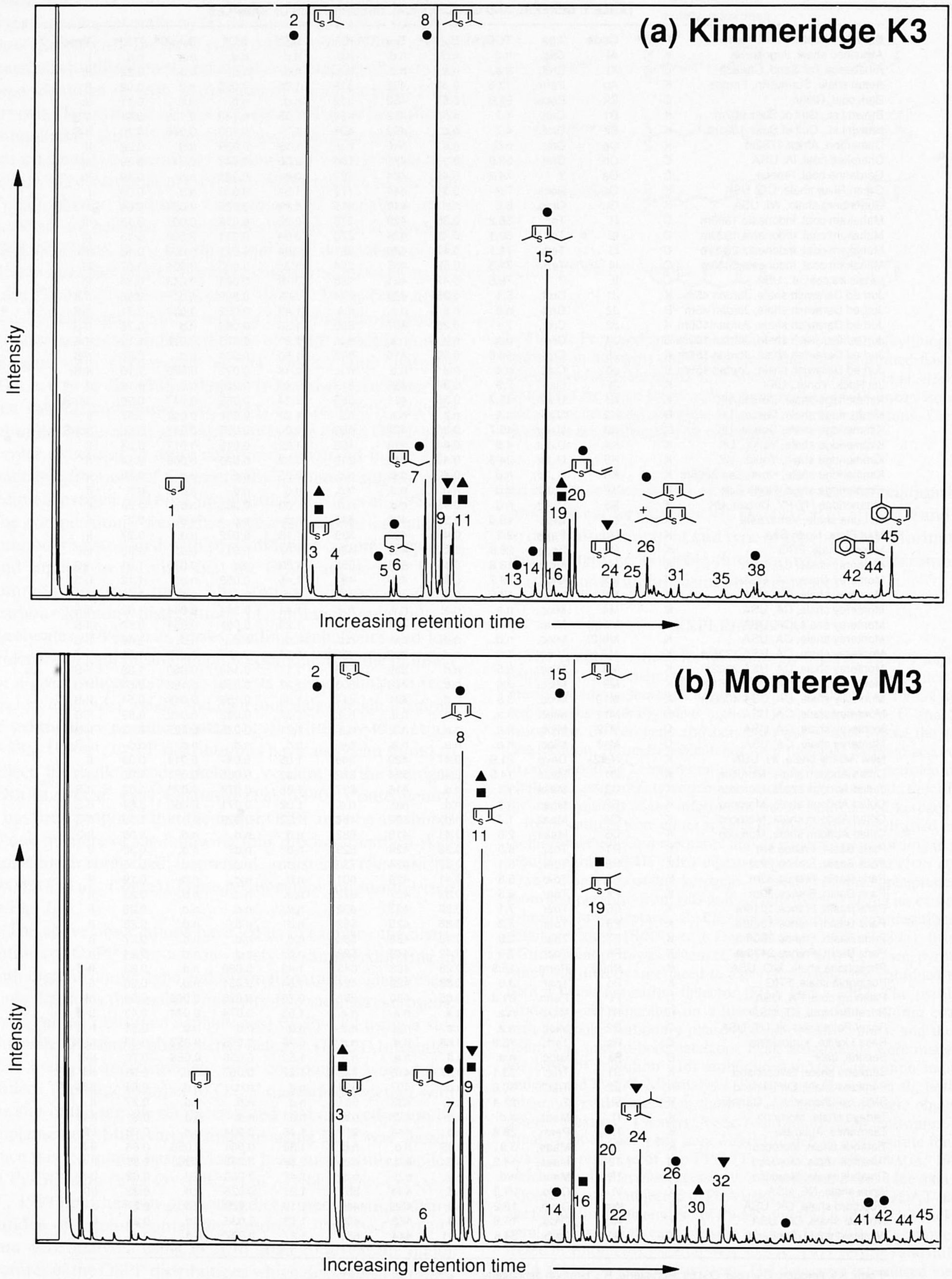

FIG. 2. FPD chromatograms of pyrolysates of four samples representing the major kerogen types: (a) Kimmeridge (Type II); (b) Monterey (Type II-S); (c) Mahakam coal (Type III); and (d) Tasmanite (Type I). For peak assignments, see Table 2. Selected structures are shown. Excluding the gas peak, all chromatograms are normalized to the second largest peak. Inferred structural relationships are indicated for major components derived from linear (solid circles), isoprenoid (solid triangles), branched (solid squares), and steroid (inverted triangles) carbon skeletons.

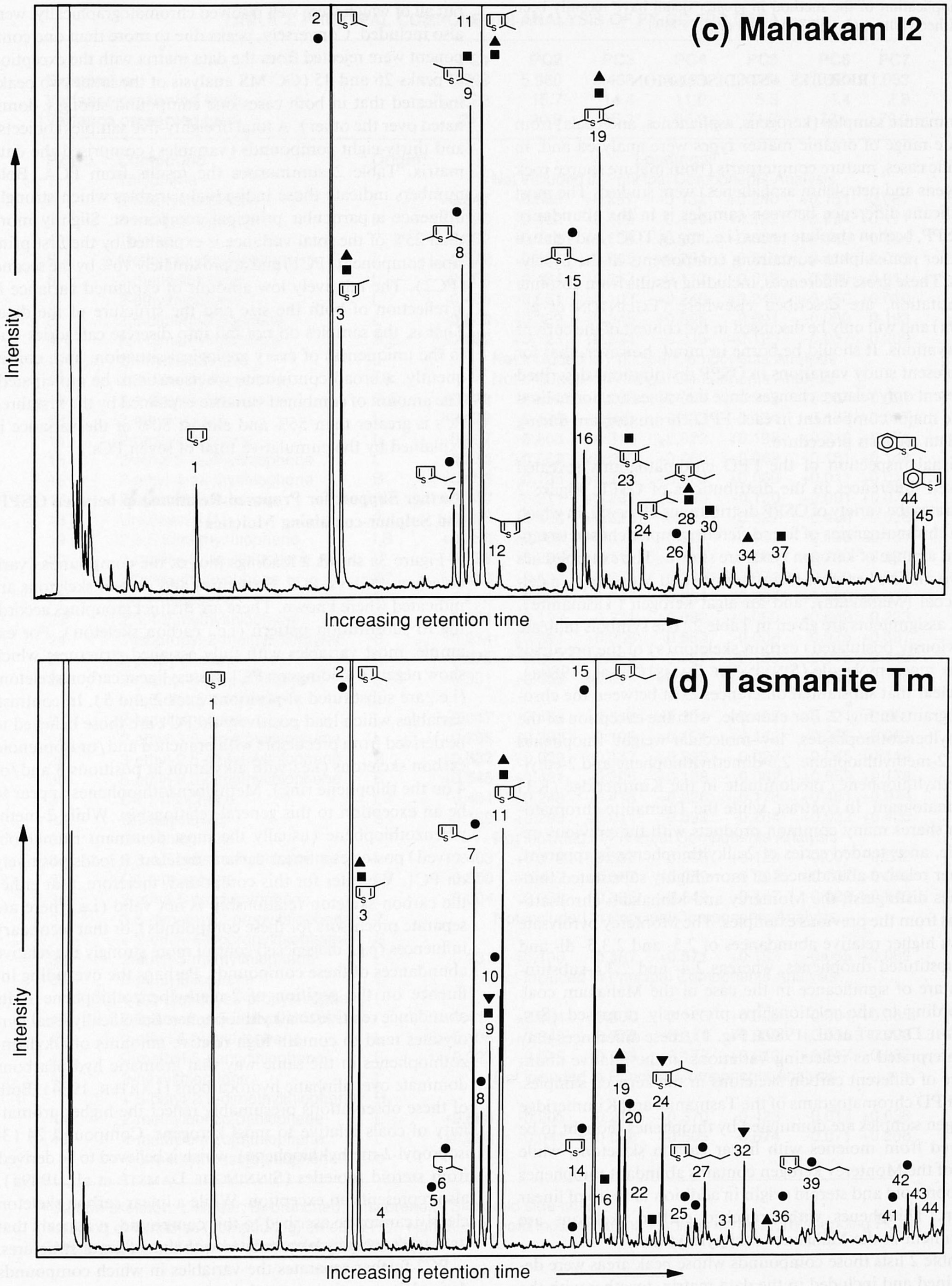

FIG. 2. (Continued)

the application of the method in greater detail have recently been published (NIP et al., 1988, MOERS et al., 1989).

RESULTS AND DISCUSSION

Immature samples (kerogens, asphaltenes, and coals) from a wide range of organic matter types were analysed and, in specific cases, mature counterparts (both mature source rock kerogens and petroleum asphaltenes) were studied. The most significant difference between samples is in the abundance of OSPP, both in absolute terms (i.e., mg/g TOC) and relative to other non-sulphur-containing components in the pyrolysates. These gross differences, including results from absolute quantitation, are described elsewhere (EGLINTON et al., 1990a) and will only be discussed in the context of the current observations. It should be borne in mind, however, that for the present study variations in OSPP distributions described represent only relative changes since the values are normalised to the major component in each FPD chromatogram during the data analysis procedure.

Visual inspection of the FPD chromatograms revealed marked differences in the distributions of OSPP. Figure 2 illustrates the variety of OSPP distributions observed, in which FPD chromatograms of four different samples chosen to represent a range of kerogen types are shown. The examples are of two marine kerogens (Kimmeridge and Monterey), a deltaic coal (Mahakam), and an algal kerogen (Tasmanite). Peak assignments are given in Table 2. The symbols indicate (previously postulated) carbon skeleton(s) of the precursor in the macromolecule (SINNINGHE DAMSTÉ et al., 1989a). It is clear that substantial differences exist between the chromatograms in Fig. 2. For example, with the exception of the methylbenzothiophenes, low-molecular-weight thiophenes (esp. 2-methylthiophene, 2,5-dimethylthiophene and 2-ethyl-5-methylthiophene) predominate in the Kimmeridge (K3) chromatogram. In contrast, while the Tasmanite chromatogram shares many common products with the previous example, an extended series of 2-alkylthiophenes is apparent. Higher relative abundances of more highly substituted thiophenes distinguish the Monterey and Mahakam chromatograms from the previous examples. The Monterey pyrolysate shows higher relative abundances of 2,3- and 2,3,5- di- and tri-substituted thiophenes, whereas 2,4- and 2,3,4-substitutions are of significance in the case of the Mahakam coal. According to the relationships previously proposed (SINNINGHE DAMSTÉ et al., 1989a; Fig. 1), these differences may be interpreted as reflecting variations in the relative abundance of different carbon skeletons in the kerogen samples. The FPD chromatograms of the Tasmanite and Kimmeridge kerogen samples are dominated by thiophenes thought to be derived from moieties with linear carbon skeletons, while that of the Monterey kerogen contains abundant thiophenes of isoprenoid and steroid origin in addition to those of linear origin. Thiophenes with branched carbon skeletons are prominent in the Mahakam coal pyrolysate.

Table 2 lists those compounds whose peak areas were determined and included in the data matrix, together with the inferred carbon skeleton of the sulphur-containing moiety attached to the macromolecule (see SINNINGHE DAMSTÉ et al., 1989a). A number of compounds of unknown structure, but all of which were well resolved chromatographically, were also included. Conversely, peaks due to more than one component were rejected from the data matrix with the exception of peaks 26 and 45 (GC-MS analysis of the latter two peaks indicated that in both cases one compound strongly dominated over the other). A total of eighty-five samples (objects) and thirty-eight compounds (variables) comprised the data matrix. Table 2 summarises the results from PCA. Bold numbers indicate those individual variables which strongly influence a particular principal component. Slightly more than 25% of the total variance is explained by the first principal component (PC1) and approximately 16% by the second (PC2). The relatively low amount of explained variance is a reflection of both the size and the structure of the data. That is, the samples do not fall into discrete categories due to the uniqueness of every geological situation, and, consequently, a broad continuous spectrum is to be anticipated. The amount of combined variance explained by the first three PCs is greater than 55% and almost 80% of the variance is explained by the cumulative total of seven PCs.

Further Support for Proposed Relationship between OSPP and Sulphur-containing Moieties

Figure 3a shows a loadings plot of the compounds (variables) on PC1 vs. PC2. Structures and carbon skeletons are indicated where known. There are distinct groupings according to substitution pattern (i.e., carbon skeleton). For example, most variables with fully assigned structures which show negative loadings on PC1 possess linear carbon skeletons (i.e., are substituted at positions 2, or 2 and 5). In contrast, variables which load positively on PC1 are those believed to be derived from precursors with branched and/or isoprenoid carbon skeletons (i.e., with alkylation at positions 3 and/or 4 on the thiophene ring). Methylbenzothiophenes appear to be an exception to this general relationship. While 2-methylbenzothiophene (usually the most dominant isomer observed) possesses a linear carbon skeleton, it loads positively on PC1. We infer for this compound, therefore, that either the carbon skeleton relationship is not valid (i.e., there are separate precursors for these compounds), or that secondary influences (e.g., diagenesis) control more strongly the relative abundances of these compounds. Perhaps the overriding influence on the position of 2-methylbenzothiophene is its abundance relative to alkylthiophenes. Specifically, coal pyrolysates tend to contain high relative amounts of alkylbenzothiophenes in the same way that aromatic hydrocarbons dominate over aliphatic hydrocarbons (LARTER, 1984). Both of these observations presumably reflect the higher aromaticity of coals relative to most kerogens. Compound 24 (3-isopropyl-2-methylthiophene), which is believed to be derived from steroid moieties (SINNINGHE DAMSTÉ et al., 1989a), also represents an exception. While a linear carbon skeleton clearly cannot be ascribed to this compound, it appears that its abundance may be correlated with that of linear structures.

PC2 further separates the variables in which compounds derived from moieties containing isoprenoid carbon skeletons (positive loadings) are distinguished from those derived from branched carbon skeletons (negative loadings). This also agrees with previous observations (SINNINGHE DAMSTÉ et

TABLE 2. PRINCIPAL COMPONENTS ANALYSIS OF PY-GC-FPD DATA

			PC1	PC2	PC3	PC4	PC5	PC6	PC7
Eigenvalue			9.599	5.960	5.468	4.183	2.022	1.680	1.053
Variance preserved each			25.3	15.7	14.4	11.0	5.3	4.4	2.8
Variance preserved total			25.3	40.9	55.3	66.3	71.7	76.1	78.9
Pk No.	**Compound**	**Origin[a]**	**Loadings[b]**						
1	Thiophene	?	Not included in Principal Components Analysis						
2	2-methylthiophene	L	**-0.547**	**-0.585**	+0.287	-0.132	+0.240	+0.151	-0.087
3	3-methylthiophene	I	+0.393	-0.422	+0.435	-0.429	+0.132	+0.094	+0.171
4	Thiolane	?	-0.152	**-0.715**	+0.109	+0.271	-0.301	-0.139	-0.164
5	Methyldihydrothiophene	L	-0.372	-0.469	+0.065	-0.261	-0.319	-0.414	-0.020
6	2-methylthiolane	L	-0.300	-0.484	-0.347	-0.117	-0.012	**-0.630**	+0.014
7	2-ethylthiophene	L	-0.455	**-0.651**	+0.103	+0.245	+0.245	+0.150	+0.010
8	2,5-dimethylthiophene	L	**-0.660**	+0.389	+0.345	+0.395	-0.091	-0.080	-0.193
9	2,4-dimethylthiophene	B,S	**+0.682**	+0.123	**+0.534**	-0.235	+0.129	-0.037	-0.209
10	2-vinylthiophene	L	Not included in Principal Components Analysis						
11	2,3-dimethylthiophene	I,B	Not included in Principal Components Analysis						
12	3,4-dimethylthiophene	B,S	**+0.823**	-0.250	+0.236	+0.001	-0.043	+0.087	-0.027
13	2-ethylthiolane	L	-0.078	-0.406	**-0.603**	-0.103	-0.134	-0.177	+0.037
14	2-propylthiophene	L	-0.097	**-0.668**	-0.312	+0.022	+0.198	+0.219	+0.276
15	2-ethyl-5-methylthiophene	L	**-0.575**	**+0.662**	+0.296	+0.069	+0.069	-0.181	+0.144
16	2-ethyl-4-methylthiophene	B	**+0.855**	-0.195	+0.264	+0.168	+0.069	+0.011	+0.014
17	Ethylmethylthiophene	B?	**+0.747**	-0.211	+0.261	+0.303	-0.120	+0.091	+0.073
18	Unknown (U1)	?	-0.055	-0.166	**-0.693**	-0.261	+0.027	-0.466	-0.026
19	2,3,5-trimethylthiophene	I,B	+0.356	**+0.799**	-0.229	-0.227	+0.132	-0.105	-0.161
20	2-methyl-5-vinylthiophene	L	**-0.778**	+0.232	-0.111	-0.099	-0.289	+0.290	-0.192
21	Ethylmethylthiophene	B?	**+0.629**	-0.192	-0.271	-0.232	-0.372	+0.269	-0.190
22	C3:1-thiophene	?	+0.216	-0.305	-0.347	**-0.534**	-0.286	+0.180	+0.052
23	2,3,4-trimethylthiophene	B,S	**+0.854**	+0.193	-0.231	-0.082	+0.069	+0.042	-0.223
24	3-isopropyl-2-methylthiophene	S	-0.234	+0.391	+0.266	**-0.653**	-0.006	-0.075	+0.397
25	2-propylthiolane	L	**-0.576**	-0.267	**-0.569**	-0.067	-0.189	-0.015	-0.140
26	2-methyl-5-propylthiophene	L	-0.351	**+0.559**	+0.021	**+0.589**	+0.119	-0.153	+0.140
	+ 2,5-diethylthiophene[m]	L							
27	2-butylthiophene	L	+0.047	-0.466	**-0.510**	+0.309	+0.407	+0.221	+0.263
28	2-ethyl-3,5-dimethylthiophene	I	**+0.705**	+0.382	-0.195	+0.151	+0.162	-0.256	+0.063
29	3-ethyl-2,5-dimethylthiophene	B	**+0.832**	+0.029	-0.147	+0.398	-0.027	-0.045	+0.112
30	5-ethyl-2,3-dimethylthiophene	B	**+0.546**	+0.421	-0.205	+0.128	-0.082	+0.059	+0.178
31	C4:1-thiophene	L?	-0.484	+0.248	-0.418	+0.026	-0.178	+0.481	+0.074
32	Unknown (U2)	S?	-0.120	+0.293	+0.011	**-0.699**	-0.264	+0.032	+0.435
33	C4:1-thiophene	?	Not included in Principal Components Analysis						
34	2,3,4,5-tetramethylthiophene	I	+0.403	+0.378	**-0.597**	-0.286	+0.128	-0.007	-0.232
35	C4:1-thiophene	L?	**-0.550**	+0.447	+0.027	+0.059	-0.397	+0.207	-0.043
36	2-ethyl-5-propylthiophene	L	-0.004	+0.238	-0.335	**+0.649**	-0.147	-0.029	+0.143
37	3,5-dimethyl-2-propylthiophene	?	Not included in Principal Components Analysis						
	+ 2-ethyl-4-isopropylthiophene	S							
38	2-butyl-5-methylthiophene	L	-0.231	+0.100	-0.487	**+0.571**	+0.183	-0.065	+0.089
39	2-pentylthiophene	L	Not included in Principal Components Analysis						
	+ 2,3-dimethyl-5-propylthiophene	I							
40	2,3-dimethyl-5-isobutylthiophene	I	+0.413	+0.064	**-0.600**	-0.176	+0.025	-0.004	+0.085
41	2-ethyl-5-butylthiophene	L	+0.108	+0.348	**-0.728**	-0.311	+0.038	+0.056	-0.023
42	2-methyl-5-pentylthiophene	L	-0.323	-0.016	**-0.729**	+0.177	+0.212	+0.217	-0.082
43	2-hexylthiophene	L	Not included in Principal Components Analysis						
	+ 5-butyl-2,3-dimethylthiophene	B							
44	2-methylbenzo[b]thiophene	L	**+0.660**	-0.205	-0.214	+0.370	-0.423	-0.017	+0.038
45	4-methylbenzo[b]thiophene	L	+0.283	-0.041	+0.076	**+0.505**	**-0.674**	-0.071	+0.208
	+ 3-methylbenzo[b]thiophene[m]	B							

[a]Carbon skeleton: L=linear; B=branched; I=isoprenoid; S=steroid side-chain.
[b]Loading of variables (compounds) on each PC. Numbers in **bold** indicate strong loadings on the corresponding PC.
[m]Minor component of peak (determined by GC-MS).

al., 1989a). In addition, a further separation of those thiophenes derived from linear carbon skeletons is apparent. Linear thiophenes substituted both at positions 2 and 5 show positive loading on PC2, whereas the mono-substituted 2-*n*-alkylthiophenes and 2-*n*-alkylthiolanes are negatively loaded on this PC.

A loadings plot (variables) of PC2 (ca. 16% of variance) vs. PC3 (ca. 14% of variance) (Fig. 4a) reveals further

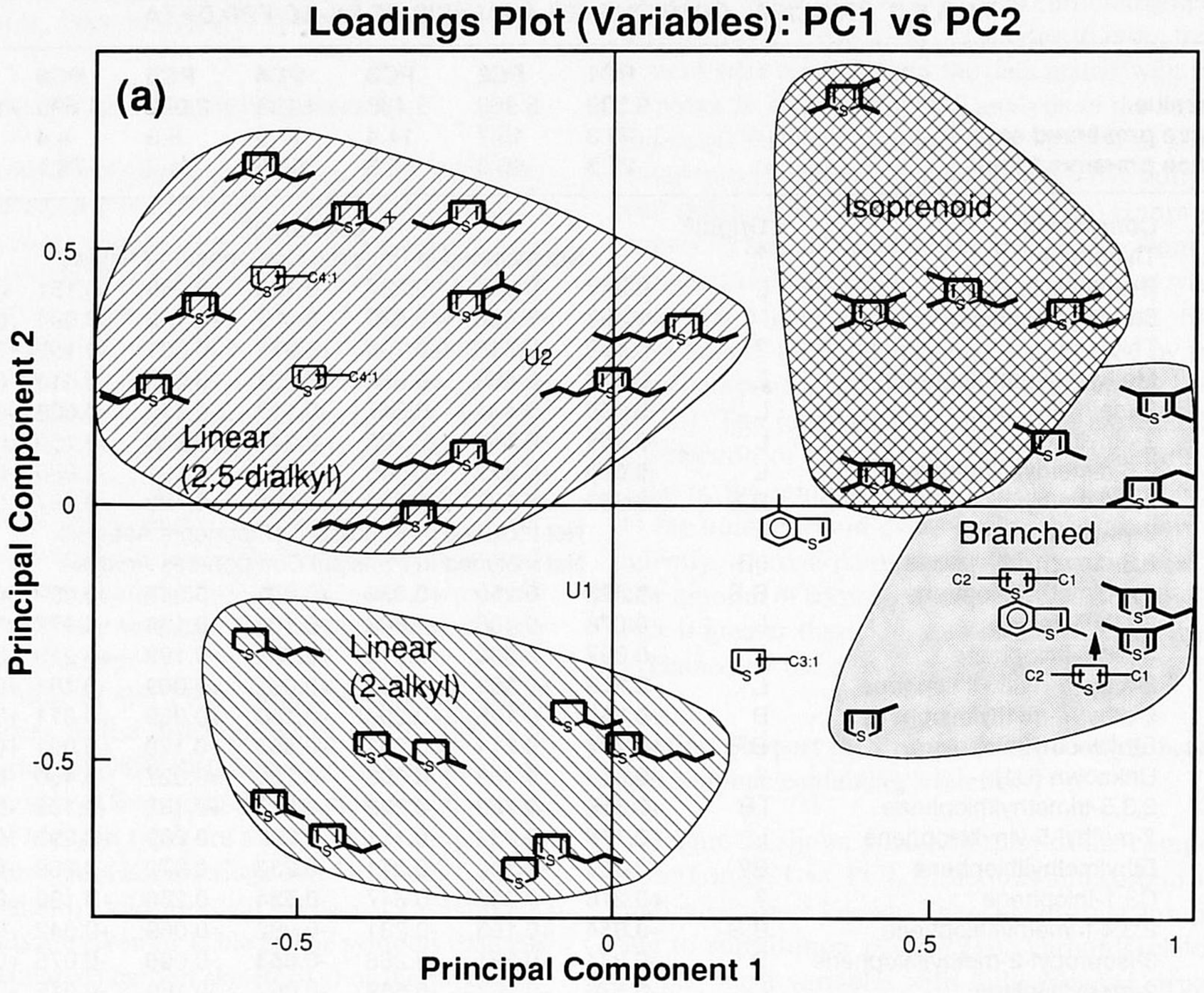

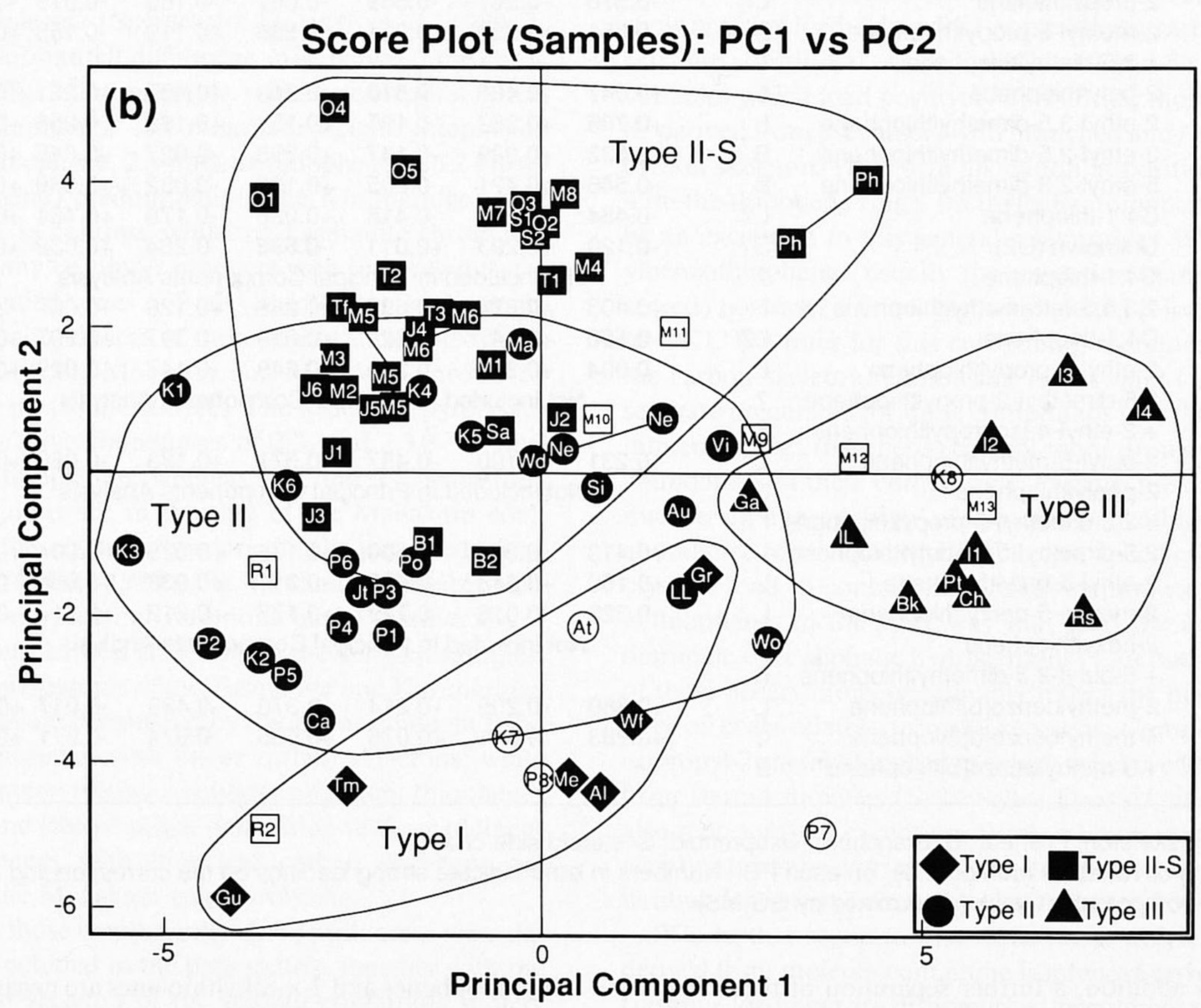

FIG. 3. (a) Plot of PC 1 vs. PC 2 showing the loadings of individual variables (compounds) on these two PCs. Carbon skeletons are indicated as bold lines. (b) Plot of PC 1 vs. PC 2 showing the scores of individual objects (samples). Immature samples ($R_0 < 0.5\%$) are indicated with solid symbols; samples from mature source rocks (R_0

structure in the data. There is a general trend of increasing alkyl carbon number with increasing "negativity" on PC3. This trend, which is most apparent within a particular homologous series (e.g., 2-*n*-alkylthiophenes), is believed to represent differences in the degree of cross-linking within the macromolecule. Namely, less extensive cross-linking gives rise to longer-chain OSPP.

One interesting additional feature of the loadings plots is that they allow some deductions to be made concerning the structure of compounds with unknown substitution patterns. For example, from Fig. 3a, it may be deduced that the two ethylmethylthiophenes (peaks 17 and 21) in the lower right-hand area of the plot almost certainly have a branched carbon skeleton origin, whereas the $C_{4:1}$ thiophenes (peaks 31 and 35) in the upper left quadrant may be assumed to be derived from precursors with linear carbon skeletons. The covariance of unknown "U2" (peak 32) with 3-isopropyl-2-methylthiophene (peak 24) similarly implies a steroid origin for the former.

Influence of Kerogen Type on OSPP Distributions

The score plots show the location of the samples (objects) with respect to the principal components. In Fig. 3b (PC1 vs. PC2), the four general kerogen types are indicated and are assigned according to elemental composition (i.e., atomic H/C, O/C, and S/C ratios) and/or programmed pyrolysis parameters (i.e., "Rock-Eval" Hydrogen Indices; Table 1) (TISSOT and WELTE, 1984). Typically, three kerogen types are distinguished: Type I (hydrogen-rich, predominantly algal or bacterial source, typically deposited under lacustrine or certain restricted marine conditions); Type II (moderately hydrogen-rich, mainly phytoplanktonic material of marine origin); and Type III (hydrogen-poor, oxygen-rich, predominantly terrestrial higher plant). A further subclassification for Type II kerogens was proposed by ORR (1984) which distinguishes organic sulphur-rich kerogens ("Type II-S"; $S_{org}/C > 0.04$). The latter are believed to arise under certain marine (e.g., upwelling environments) or hypersaline conditions. Figure 3b suggests that the OSPP distributions are related to kerogen type. PC1 distinguishes the Type III kerogens (mainly coals) from the Types I, II and II-S. A gradation from Type II-S (positive) → II → I (negative) is apparent on PC2. Samples from similar stratigraphic or areal locations (i.e., representing similar depositional environments) such as those from the Mahakam Delta (I), Paris Basin (P), and Oulad-Abdoun (O) each cluster within their broad kerogen types. Similarly, on the basis of this plot, Toarcian kerogens from the Paris Basin (France) show similar characteristics to those from the stratigraphically equivalent Posidonia shale (Po) of western Germany.

Comparison of the sample positions in the score plots with the corresponding loadings plots allows several deductions to be made regarding assignment of those OSPP which are characteristic for certain kerogen types. Regarding PC1, it is evident that the coals are distinguished by higher relative amounts of branched and, to some extent, isoprenoid thiophenes (Fig. 3a). This is clearly seen in the FPD chromatogram (Fig. 2) of the Mahakam coal pyrolysate. In contrast, Type I-II kerogens show a higher relative abundance of thiophenes derived from precursors with linear carbon skeletons in their pyrolysates (e.g., Kimmeridge; Fig. 2). The distinction between Type II-S and Type I kerogens (Type II being intermediate in this gradation) in PC2 is thought to be a result of the differences in the types of linear thiophenes as well as the abundance of isoprenoid thiophenes. Type I kerogens show a higher relative abundance of 2-*n*-alkylthiophenes as exemplified by the FPD chromatogram of the flash pyrolysate of the Tasmanite kerogen. In contrast, the Type II-S kerogen pyrolysates show a higher relative abundance of 2,5-di-substituted thiophenes, together with higher abundances of isoprenoid and/or steroid thiophenes (cf. Monterey kerogen; Fig. 2). Of the Type II-S kerogens, the Phosphoria retort shale is particularly rich in isoprenoid thiophenes (SINNINGHE DAMSTÉ et al., 1989a).

One thiophene which appears to be particularly characteristic for Type II-S kerogens from the Phosphoria shale and phosphatic horizons in other sulphur-rich shales (e.g., Oulad Abdoun, Timahdit, Tarfaya, Jurf ed Darawish, and Monterey) is 2,3,4,5-tetramethylthiophene (peak 34). As an example, Fig. 5 shows FPD chromatograms of kerogens from a bituminous and a phosphatic zone within the Cretaceous Timahdit Formation (Morocco). The tetramethylthiophene is considered to be a pyrolysis product of highly branched isoprenoid thiophenic moieties for the following reason: Diatoms, which flourish under the upwelling conditions believed to be responsible for certain phosphatic deposits, are known to contain highly branched hydrocarbons. Sulphur-containing equivalents (i.e., with identical carbon skeletons) have been identified in sediment extracts for some of the samples analysed herein (SINNINGHE DAMSTÉ et al., 1989c,d; 1990b; KOHNEN et al., 1990a) and have been attributed to the incorporation of sulphur into the corresponding functionalised hydrocarbons (KOHNEN et al., 1990b; SINNINGHE DAMSTÉ et al., 1990b). We conclude, therefore, that 2,3,4,5-tetramethylthiophene could be a likely pyrolysis product of such highly branched isoprenoid thiophene moieties incorporated into the kerogen. It is also notable in this respect that two other likely products from pyrolysis of sulfur-containing moieties containing highly branched isoprenoid carbon skeletons, namely 2-ethyl-3,4,5-trimethylthiophene and 3-ethyl-2,4,5-trimethylthiophene (Peaks X and Y, respectively; Fig. 5b), also show increased prominence paralleling the tetramethylthiophene.

It must be borne in mind that the absolute yields of sulphur compounds from pyrolysates vary dramatically depending on kerogen type (EGLINTON et al., 1990a). The abundance of sulphur compounds in kerogens pyrolysates may be

---

> 0.5%) and oils are shown with open symbols. For explanation of code within symbols, see Table 1. The four major kerogen types are indicated as diamonds (Type I), circles (Type II), squares (Type II-S), and triangles (Type III). "Clouds" enclosing each kerogen type are drawn on the basis of immature samples only. Replicate analyses are represented by interconnected symbols. For sample M5, this represents analysis of an unextracted rock, an extracted rock, and an isolated kerogen.

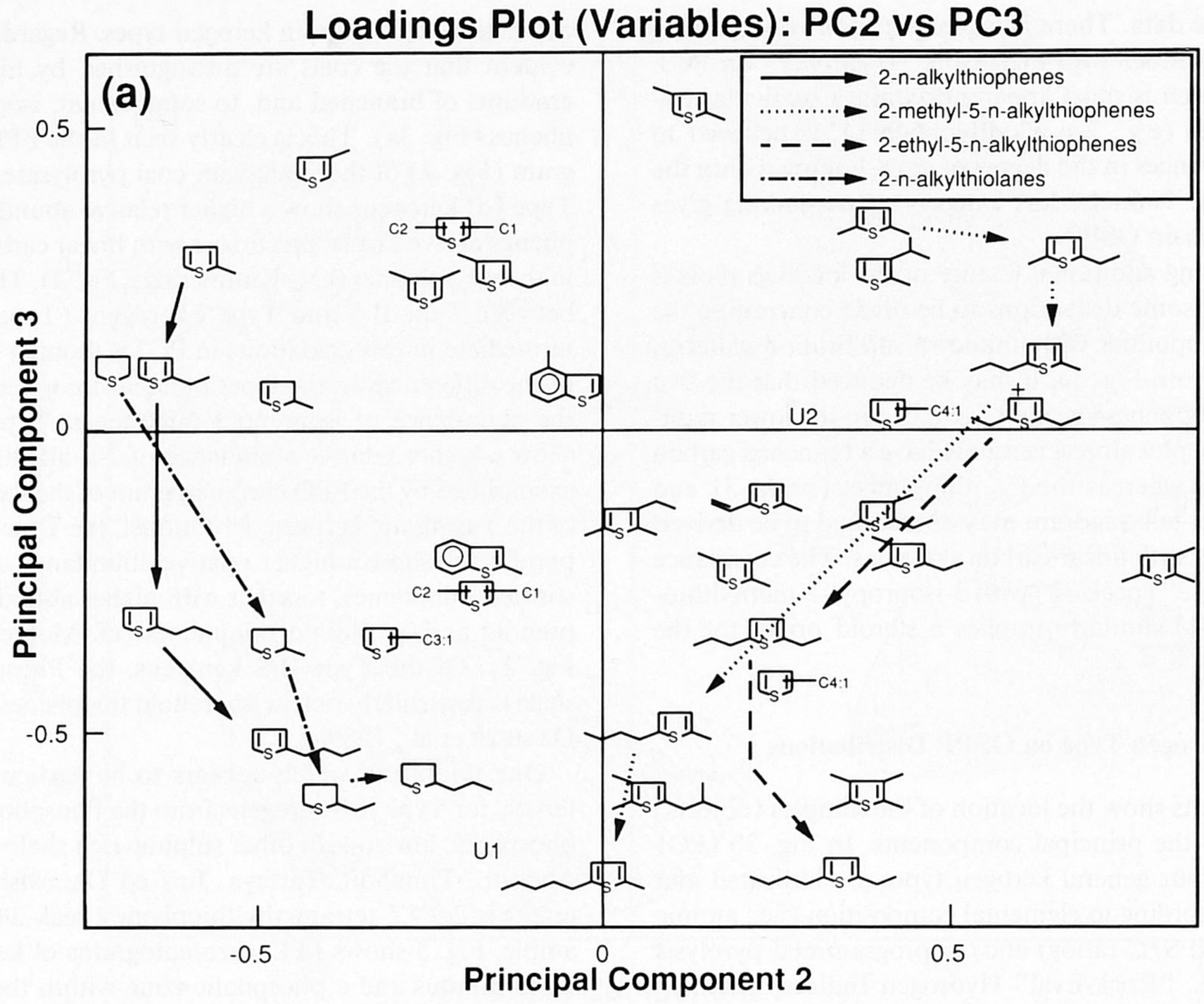

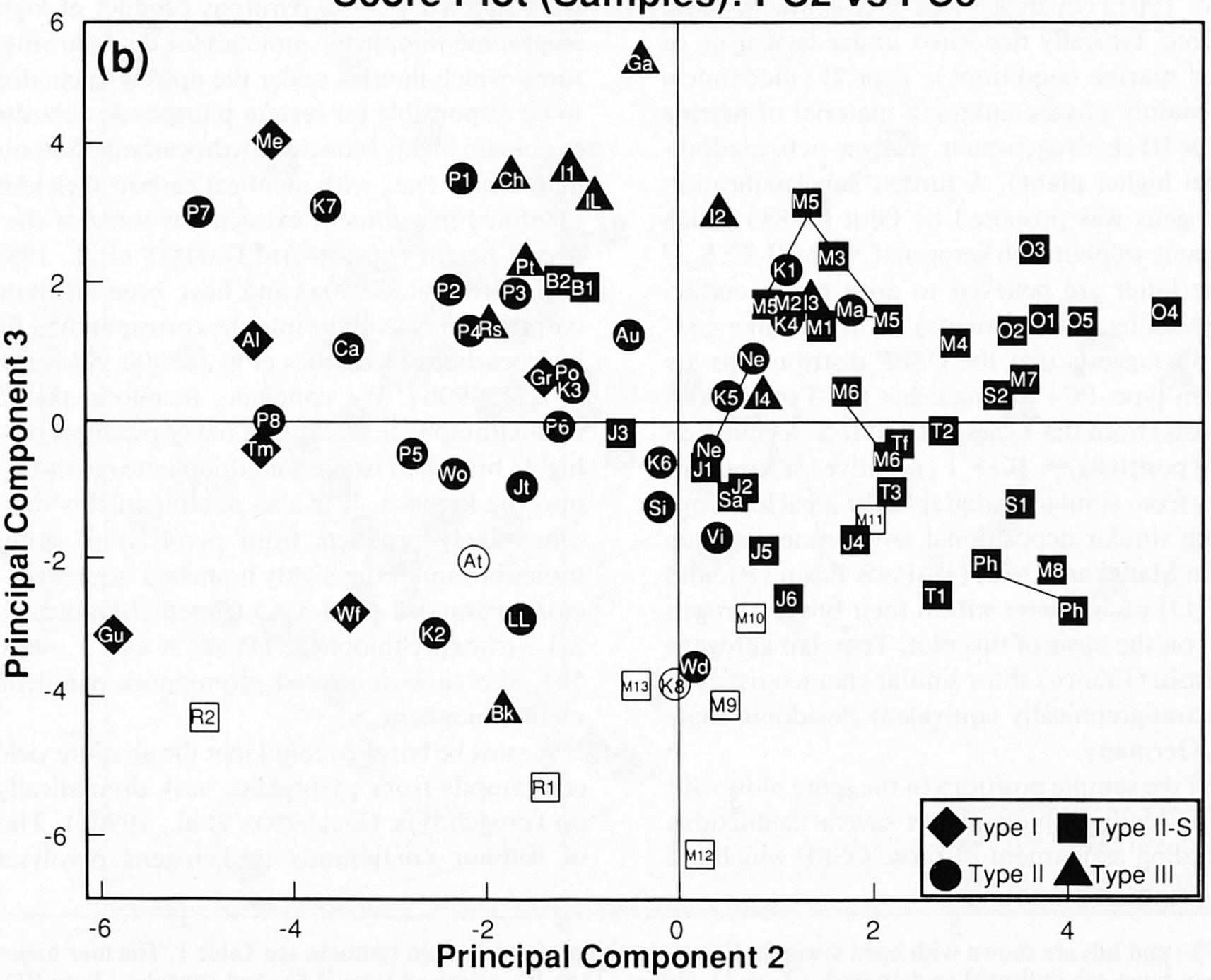

FIG. 4. (a) Plot of PC 3 vs. PC 2 showing the loadings of individual variables (compounds) on these two PCs. Arrows indicate homologous series increasing in alkyl chain length. (b) Plot of PC 3 vs. PC 2 showing the scores of individual objects (samples) on these two PCs. Symbol key and explanation as for Fig. 3b.

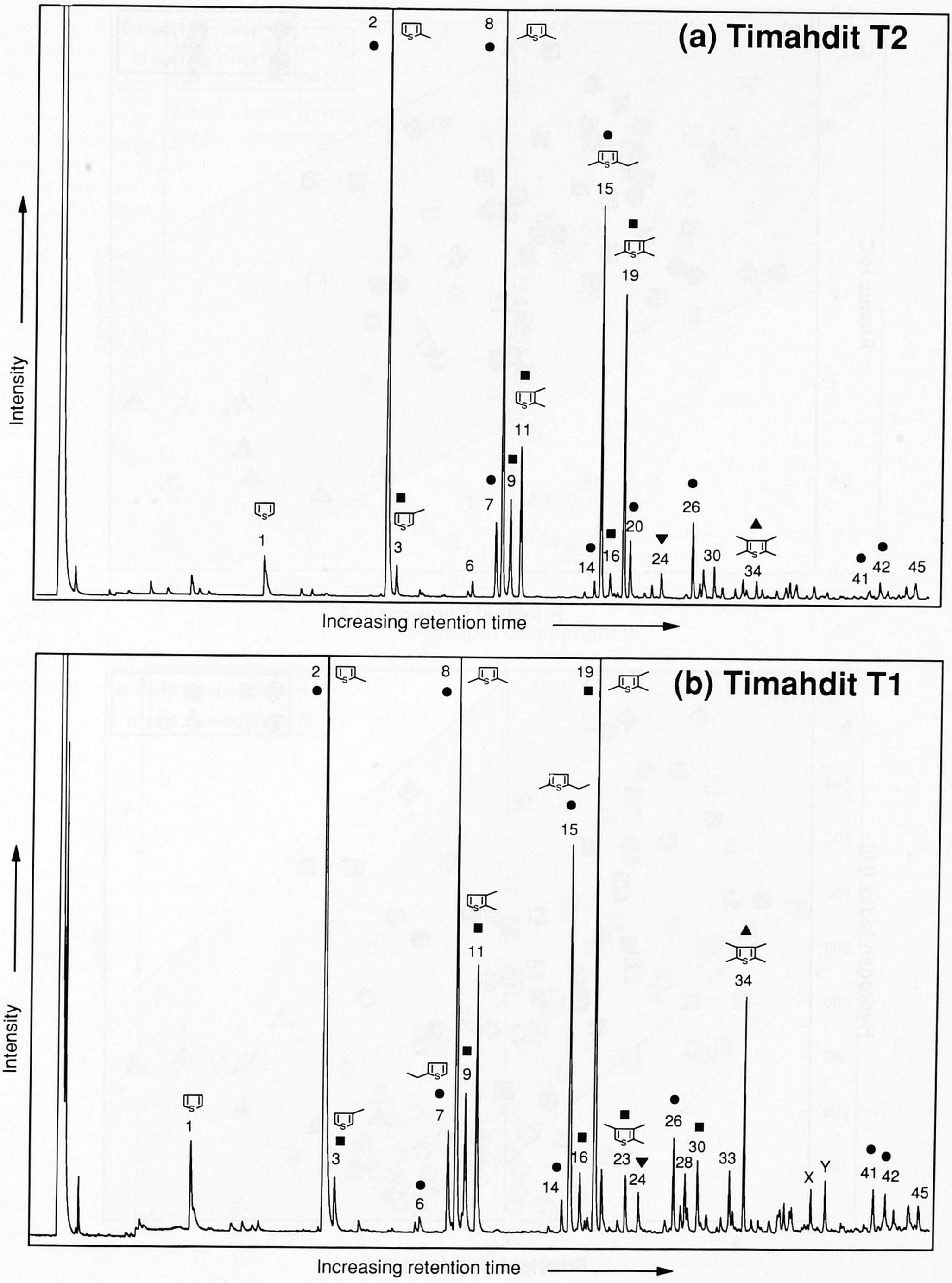

FIG. 5. FPD chromatograms of pyrolysates of two kerogen samples from the Timahdit Formation (Morocco): (a) Bituminous zone; (b) Phosphatic zone. For peak assignments, see Table 2. Selected structures are shown. Excluding the gas peak, all chromatograms are normalized to the second largest peak. See Fig. 2 for explanation of symbols. Peaks X and Y correspond to 2-ethyl-3,4,5-trimethylthiophene and 3-ethyl-2,4,5-trimethylthiophene, respectively.

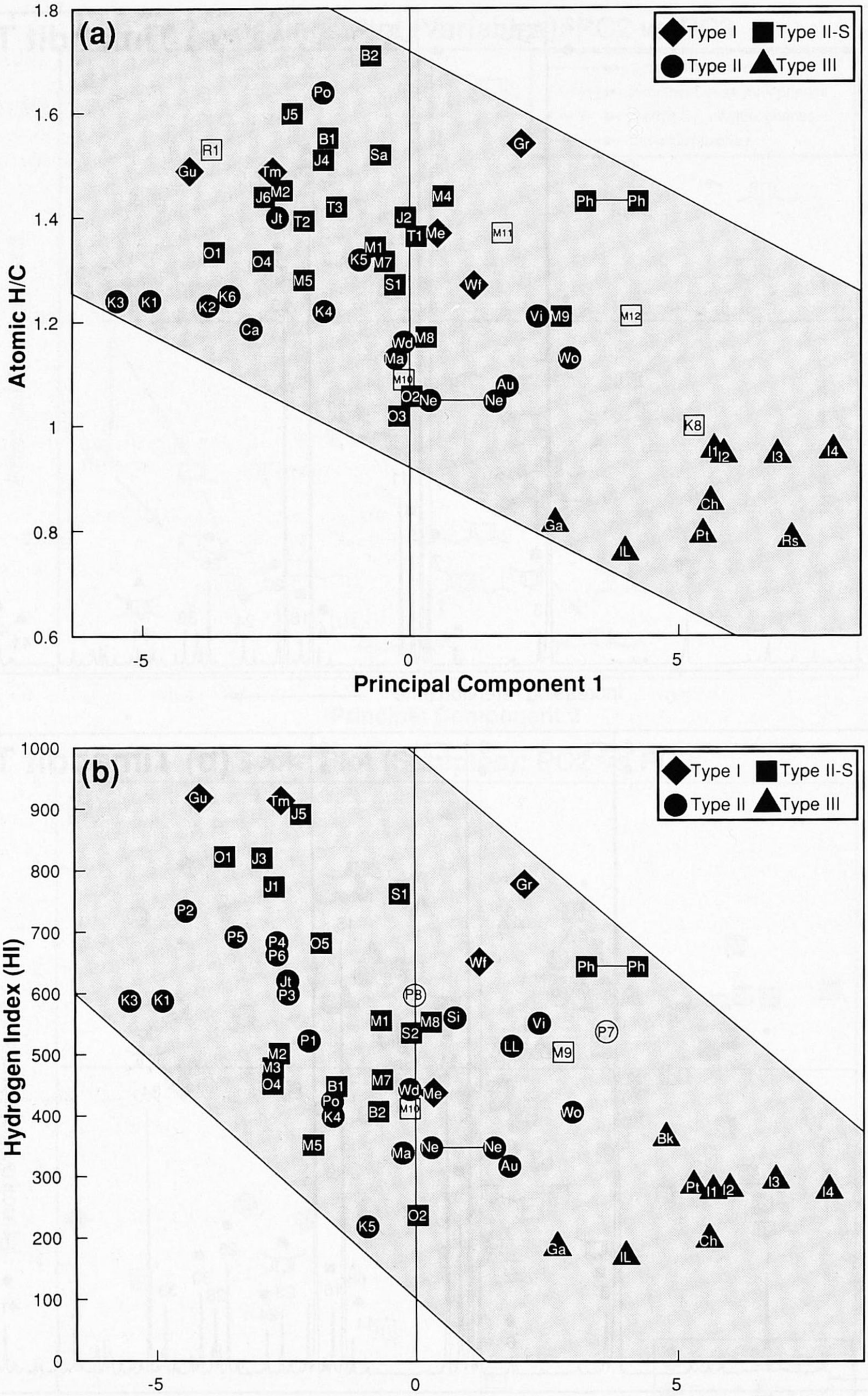

FIG. 6. (a) Relationship between atomic H/C ratio and PC 1. (b) Relationship between Rock-Eval Hydrogen Index (HI) and PC 1. Symbol key and explanation as for Fig. 3b.

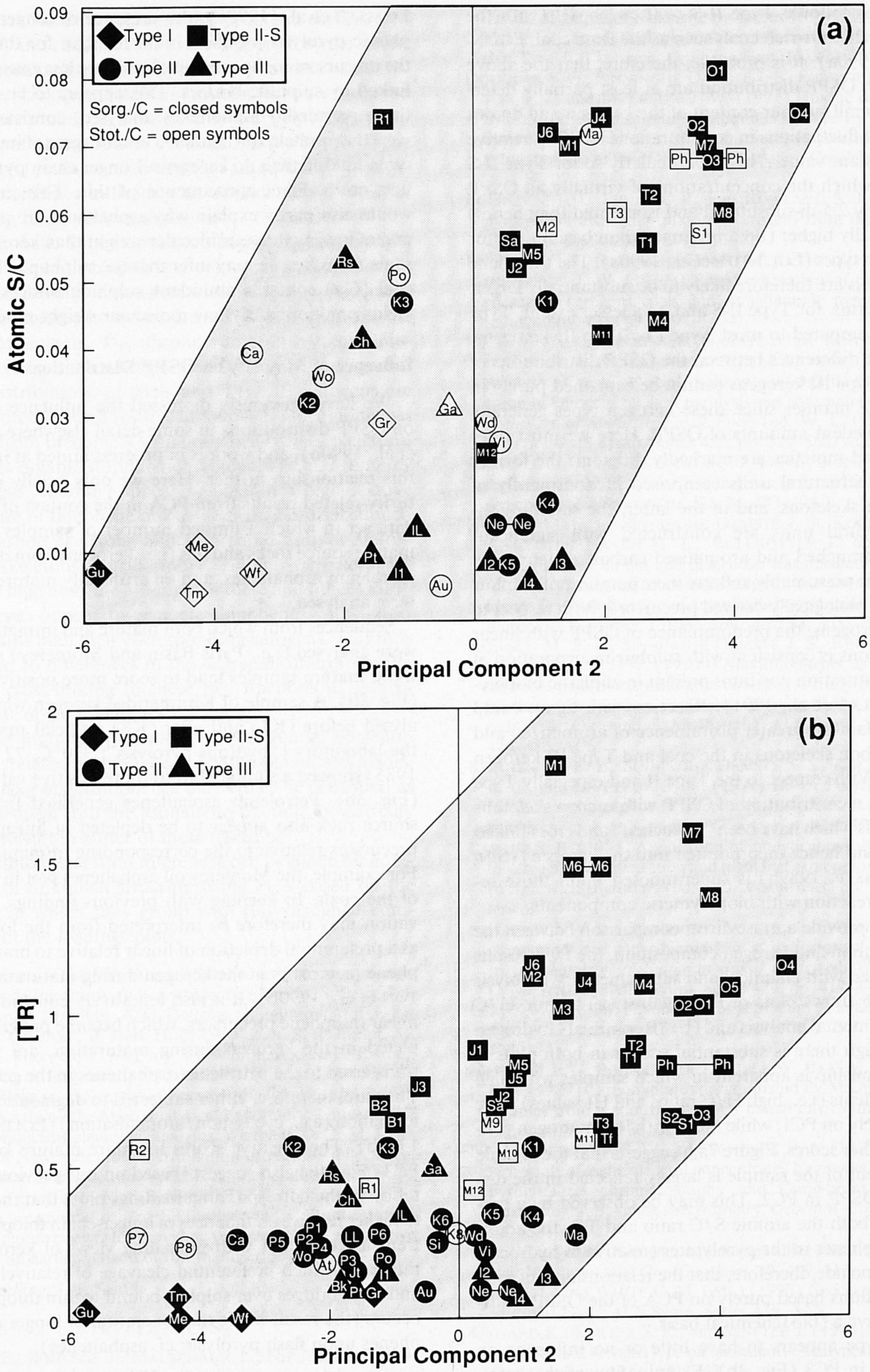

FIG. 7. (a) Relationship between atomic S/C ratio and PC 2. Open and closed symbols refer to determinations of S_{total}/C and $S_{organic}/C$, respectively. (b) Relationship between TR, determined from flash pyrolysis (=[2,3-dimethylthiophene]/[*n*-non-1-ene plus 1,2-dimethylbenzene]) and PC 2. For symbol key and explanation, see Fig. 3b and Table 1.

generalised as follows: Type II-S > II > I = III (with the exception of sulphur-rich coals such as the Rasa coal; EGLINTON et al., 1990a). It is probable, therefore, that the above differences in OSPP distribution are at least partially determined by overall sulphur content of the kerogen and do not merely reflect fluctuations in concentrations of OSPP relative to some constant value. This is particularly so for Type II-S kerogens in which the concentrations of virtually all OSPP (and especially 2,5-di-substituted and isoprenoid thiophenes) are substantially higher (on a per mg carbon basis) than for other kerogen types (EGLINTON et al., 1990a). The thiophene precursor pools are therefore likely to be substantially larger, in absolute terms, for Type II-S and, to a lesser extent, Type II kerogens compared to most Type I or Type III kerogens. However, the differences between the OSPP distributions of Type I and Type III kerogens cannot be explained purely in a quantitative manner since these kerogen types generally produce equivalent amounts of OSPP. Here we must infer that the bound moieties are markedly different, the former consisting of structural units comprised predominantly of linear carbon skeletons; and in the latter, the sulphur-containing structural units are constructed with significant amounts of branched and aromatised carbon skeletons. In each case, this presumably reflects incorporation of sulphur into different biologically derived precursors. With respect to the Type I kerogens, the predominance of OSPP with linear carbon skeletons is consistent with sulphur incorporation at terminal unsaturation positions present in aliphatic biopolymers (DOUGLAS et al., 1991). Reaction with lignin could similarly explain the greater prominence of aromatized and branched carbon skeletons in the coal and Type III kerogen pyrolysates. With respect to the Type II and especially Type II-S kerogens, a contribution of OSPP with carbon skeletons reflecting lipids which have been "quenched" and cross-linked by sulphur (and hence incorporated into the kerogen) (SINNINGHE DAMSTÉ, 1989b) is superimposed upon those resulting from reaction with biopolymeric components.

In order to provide a more direct comparison between the OSPP distribution and kerogen composition, the PCA results were contrasted with chemical and supplementary pyrolysis data. Figure 6 shows plots of PC1 against (a) atomic H/C ratio from elemental analysis and (b) "Rock-Eval" hydrogen index. Although there is substantial scatter in both plots, a general relationship is apparent in which samples with high hydrogen contents (i.e., high H/C ratios and HI values) score more negatively on PC1, while those with low hydrogen contents have higher scores. Figure 7a,b suggests that the organic sulphur content of the sample is largely reflected in the distribution of OSPP in PC2. This may be observed by a correlation with both the atomic S/C ratio and TR, the abundance of thiophenes in the pyrolysates (relative to hydrocarbons). We conclude, therefore, that the relationships inferred from observations based purely on PCA of the OSPP distributions do have a (bio)chemical basis.

Kerogen type appears to have little or no influence on sample score in PC3 (Fig. 4b). Examination of the corresponding loadings plot and Table 2 indicates that the main variation is according to alkyl chain length. It may be inferred, therefore, that samples which score negatively on PC3 give rise to longer chain thiophenes. According to the models of macromolecular sulphur bonding proposed by SINNINGHE DAMSTÉ et al. (1990a), the presence of longer-chain thiophenic pyrolysis products indicates that, for these samples, the precursors in the macromolecule are less extensively cross-linked by sulphide bridges. This appears to be the case for those petroleum asphaltenes analysed, consistent with the view that asphaltenes contain a lower degree of intermolecular cross-linking than do kerogens. Longer chain pyrolysis products are a direct consequence of this. This interpretation would also partly explain why asphaltenes are more soluble and of lower average molecular weight than kerogens. By the same measure, we may infer that the sulphur-rich Gardanne coal (Ga) contains abundant sulphide bridges and hence yields predominantly low molecular weight products.

Influence of Maturity on OSPP Distributions

We have previously discussed the influence of maturity on OSPP distributions in some detail elsewhere (EGLINTON et al., 1990b), and work is in progress aimed at investigating this relationship further. Here we only briefly discuss maturity-related results from PCA in the context of the present data set in which a limited number of samples from more mature source rocks and oils (i.e., kerogens from deeper cores, petroleum asphaltenes, and an artificially matured kerogen) were analysed.

Sequences from which both mature and immature samples were analysed (i.e., Paris Basin and Monterey) suggest that more mature samples tend to score more positively on PC1 (Fig. 3b). A sample of Kimmeridge kerogen which was analysed before (K1) and after (K8) artificial maturation in the laboratory ("hydrous pyrolysis"; 330°C, 72 h; LEWAN, 1985) showed a similar shift to more positive values on PC1 (Fig. 3b). Petroleum asphaltenes generated from a given source rock also appear to be depleted in linear thiophene precursors relative to the corresponding immature kerogen. For example, the Monterey oil asphaltenes plot in the vicinity of the coals. In keeping with previous findings, this observation may therefore be interpreted from the loadings plot as a preferential depletion of linear relative to branched thiophene precursors in the kerogen during maturation (EGLINTON et al., 1990b). It is also tentatively concluded that the linear thiophene precursors, which become preferentially depleted in the kerogen during maturation, are not simply transferred to the petroleum asphaltenes in the generated oil. They are, therefore, either subjected to degradation or transformation (e.g., cyclisation/aromatisation) (EGLINTON et al., 1990b). The negative scores for more mature kerogens on PC3 (Fig. 4b) also suggest (based on our previous interpretation of the corresponding loadings plot) that they give rise to higher relative abundances of longer-chain thiophenes. This trend is consistent with prevailing views of kerogen maturation, in which preferential cleavage of relatively weak -S- and -S-S- bridges over sulphur bound within thiophene rings occurs (the result being the generation of longer chain thiophenes upon flash pyrolysis; cf. asphaltenes).

CONCLUSIONS

Consideration of the results described above in combination with previous observations allows the following conclusions to be made concerning the relative distributions of OSPP of geological macromolecules:

1) The carbon skeleton relationships proposed earlier (SINNINGHE DAMSTÉ et al., 1989a) are supported by the results from multivariate (principal components) analysis. Characteristic carbon skeleton distributions are observed which vary mainly as a function of kerogen type.
2) Typical petroleum source rocks of marine origin (Type II kerogens) produce relatively high amounts of 2-methyl-5-alkylthiophenes indicating an abundance of moieties possessing linear carbon skeletons.
3) Highly aliphatic Type I kerogens of algal or cuticular origin (i.e., high aliphatic biopolymer content; TEGELAAR et al., 1989) also liberate thiophenes with predominantly linear carbon skeletons; however, 2-*n*-alkylthiophenes are the dominant isomers. The absolute amount of these thiophenes are considerably less than for Type II kerogens.
4) OSPP distributions of coals and Type III kerogens are characterised by high relative amounts of alkylthiophenes derived from precursors with branched carbon skeletons.
5) The most organic sulphur-rich kerogens (e.g., Monterey and Oulad Abdoun) appear to contain a high relative abundance of thiophene precursors with 2,5-disubstituted linear carbon skeletons and isoprenoid and/or steroid carbon skeletons. Furthermore, sulphur-rich kerogens generate high absolute amounts of these and other OSPP.
6) Asphaltenes appear to generate thiophenes with longer alkyl chains than their corresponding kerogens. This may be related to differences in the degree of intermolecular sulphur cross-linking in these two fractions of macromolecular organic matter.
7) Increased maturation results in a preferential depletion of linear relative to branched alkylthiophene precursors. These linear alkylthiophenes may either be generated as such, partition into the asphaltene fraction, or partially aromatise within either of these fractions.
8) Some limited structural inferences can be made for compounds of unknown structure using PCA based on the manner in which they group with fully assigned compounds in the loadings plots.

Acknowledgments—The following are thanked for provision of samples which made the above study possible: P. Albrecht, S. Betts, J. J. Boon, P. Crisp, P. Donohoe, A. G. Douglas, G. Eglinton, M. Fowler, Fu Jiamo, P. Given, P. B. Hall, H. L. ten Haven, S. R. Larter, M. Lewan, J. R. Maxwell, J. McEvoy, M. Monthioux, S. E. Palmer, R. L. Patience, A. Raymond, D. Smith, N. Telnæs, J. Trichet, P. Tromp, H. Wehner, the Institute Français du Petrole, and British Petroleum. We thank the Microanalytical Laboratory, University of Bristol for conducting elemental analyses. We thank Dr. J. M. Jones (University of Newcastle) for determination of vitrinite reflectance. Lorraine Buxton is thanked for optical analyses and technical assistance. We are grateful to Math Kohnen (TU Delft) for useful discussions. We are grateful to Drs. E. Tegelaar and J. Zumberge and to one anonymous reviewer for providing very useful and constructive criticisms on an earlier version of this manuscript.

Editorial handling: J. T. Senftle

REFERENCES

BOUDOU J. P., BOULÈGE J., MALECHAUX L., NIP M., DE LEEUW J. W., and BOON J. J. (1987) Identification of some sulphur species in high organic sulphur coal. *Fuel* **66,** 1558–1569.

BRASSELL S. C., LEWIS C. A., DE LEEUW J. W., DE LANGE F., and SINNINGHE DAMSTÉ J. S. (1986) Isoprenoid thiophenes: Novel diagenetic products in sediments? *Nature* **320,** 160–162.

DERENNE S., LARGEAU C., CASADEVALL E., SINNINGHE DAMSTÉ J. S., TEGELAAR E. W., and DE LEEUW J. W. (1990) Characterization of Estonian Kukersite by spectroscopy and pyrolysis: Evidence for abundant alkylphenolic moieties in an Ordovician marine Type II/I kerogen. *Org. Geochem.* **16,** 873–888.

DOUGLAS A. G., SINNINGHE DAMSTÉ J. S., FOWLER M. G., EGLINTON T. I., and DE LEEUW J. W. (1991) Unique distributions of hydrocarbons and sulphur compounds released by flash pyrolysis from the fossilised alga *Gloeocapsomorpha prisca,* a major constituent of one of four Ordovician kerogens. *Geochim. Cosmochim. Acta* **55,** 275–291.

EGLINTON T. I., PHILP R. P., and ROWLAND S. J. (1988) Flash pyrolysis of artificially matured kerogens from the Kimmeridge Clay, UK *Org. Geochem.* **12,** 33–41.

EGLINTON T. I., SINNINGHE DAMSTÉ J. S., KOHNEN M. E. L., and DE LEEUW J. W. (1990a) Rapid estimation of organic sulphur content of kerogens, coals, and asphaltenes by pyrolysis–gas chromatography. *Fuel* **69,** 1394–1404.

EGLINTON T. I., SINNINGHE DAMSTÉ J. S., KOHNEN M. E. L., DE LEEUW J. W., LARTER S. R., and PATIENCE R. L. (1990b) Analysis of maturity-related changes in organic sulphur composition of kerogens by flash pyrolysis–gas chromatography. In *Geochemistry of Sulfur in Fossil Fuels* (ed. W. L. ORR and C. M. WHITE); ACS Symp. Series 429, pp. 529–565. ACS.

FARWELL S. O. and BARINAGA C. J. (1986) Sulphur-selective detection with the FPD: Current enigmas, practical usage, and future directions. *J. Chromatogr. Sci.* **24,** 483–494.

KOHNEN M. E. L., SINNINGHE DAMSTÉ J. S., KOCK-VAN DALEN A. C., TEN HAVEN H. L., RULLKÖTTER J., and DE LEEUW J. W. (1990a) Origin and diagenetic transformations of C_{25} and C_{30} highly branched isoprenoid sulphur compounds: Further evidence for the formation of organically bound sulphur during early diagenesis. *Geochim. Cosmochim. Acta* **54,** 3053–3063.

KOHNEN M. E. L., SINNINGHE DAMSTÉ J. S., RIJPSTRA W. I. C., and DE LEEUW J. W. (1990b) Alkylthiophenes as sensitive indicators of palaeoenvironmental changes. A study of a Cretaceous oil shale from Jordan. In *Geochemistry of Sulfur in Fossil Fuels* (ed. W. L. ORR and C. M. WHITE); ACS Symp. Series 429, pp. 444–485. ACS.

KOHNEN M. E. L., SINNINGHE DAMSTÉ J. S., KOCK-VAN DALEN A. C., and DE LEEUW J. W. (1991) Di- or Polysulphide-bound biomarkers in sulphur-rich geomacromolecules as revealed by selective chemolysis. *Geochim. Cosmochim. Acta* **55,** 1375–1394.

LARTER S. R. (1984) Application of analytical pyrolysis techniques to kerogen characterization and fossil fuel exploration/exploitation. In *Analytical Pyrolysis* (ed. K. J. VOORHEES) pp. 212–275. Butterworths.

DE LEEUW J. W. and SINNINGHE DAMSTÉ J. S. (1990) Organic sulfur compounds and other biomarkers as indicators of palaeosalinity. In *Geochemistry of Sulfur in Fossil Fuels* (ed. W. L. ORR and C. M. WHITE); ACS Symp. Series 429, pp. 417–443. ACS.

LEWAN M. D. (1985) Evaluation of petroleum generation by hydrous pyrolysis experimentation. *Phil. Trans. Roy. Soc. London* **A315,** 123–134.

MOERS M. E. C., BOON J. J., DE LEEUW J. W., BAAS M., and SCHENCK P. A. (1989) Carbohydrate speciation and Py-MS mapping of peat samples from a subtropical open marsh environment. *Geochim. Cosmochim. Acta* **53,** 2011–2021.

NIP M., DE LEEUW J. W., and SCHENCK P. A. (1988) The characterization of eight maceral concentrates by means of Curie point pyrolysis–gas chromatography and Curie-point pyrolysis–gas chromatography–mass spectrometry. *Geochim. Cosmochim. Acta* **52,** 637–648.

ORR W. L. (1984) Kerogen/asphaltene/sulfur relationships in sulfur-rich Monterey oils. *Org. Geochem.* **10,** 499–516.

ORR W. L. and WHITE C. M. (eds.) (1990) *Geochemistry of Sulfur in Fossil Fuels;* ACS Symp. Series 429. ACS.

ØYGARD K., LARTER S. R., and SENFTLE J. (1988) The control of maturity and kerogen type on quantitative analytical pyrolysis data. *Org. Geochem.* **13,** 1153–1162.

PHILP R. P., BAKEL A., GALVEZ-SINIBALDI A., and LIN L. H. (1988) A comparison of organosulphur compounds produced by pyrolysis of asphaltenes and those present in related crude oils and tar sands. *Org. Geochem.* **13,** 915–926.

RYAN-GRAY N., LANCASTER C. J., and GETHNER J. (1991) Chemometric analysis of pyrolysate compositions: A model for

predicting the organic matter type of source rocks using pyrolysis/gas chromatography. *J. Anal. Appl. Pyrol.* **20,** 87–106.

SINNINGHE DAMSTÉ J. S. (1988) Organically bound sulphur in the Geosphere: A molecular approach. Ph.D. thesis, Delft Technical University.

SINNINGHE DAMSTÉ J. S., KOCK-VAN DALEN A. C., DE LEEUW J. W., and SCHENCK P. A. (1988a) The identification of homologous series of alkylated thiophenes, thiolanes, thianes, and benzothiophenes present in pyrolysates of sulphur-rich kerogens. *J. Chromatogr.* **435,** 435–452.

SINNINGHE DAMSTÉ J. S., RIJPSTRA W. I. C., DE LEEUW J. W., and SCHENCK P. A. (1988b) Origin of organic sulphur compounds and sulphur-containing high molecular weight substances in sediments and immature crude oils. *Org. Geochem.* **13,** 593–606.

SINNINGHE DAMSTÉ J. S., EGLINTON T. I., DE LEEUW J. W., and SCHENCK P. A. (1989a) Organic sulphur in macromolecular sedimentary organic matter: I. Structure and origin of sulphur-containing moieties in kerogen, asphaltenes, and coal as revealed by flash pyrolysis. *Geochim. Cosmochim. Acta* **53,** 873–889.

SINNINGHE DAMSTÉ J. S., RIJPSTRA W. I. C., KOCK-VAN DALEN A. C., DE LEEUW J. W., and SCHENCK P. A. (1989b) Quenching of labile functionalised lipids by inorganic sulphur species: Evidence for the formation of sedimentary organic sulphur compounds at the early stages of diagenesis. *Geochim. Cosmochim. Acta* **53,** 1343–1355.

SINNINGHE DAMSTÉ J. S., VAN KOERT E. R., KOCK-VAN DALEN A. C., DE LEEUW J. W., and SCHENCK P. A. (1989c) Characterisation of highly branched isoprenoid thiophenes occurring in sediments and immature crude oils. *Org. Geochem.* **14,** 555–567.

SINNINGHE DAMSTÉ J. S., RIJPSTRA W. I. C., DE LEEUW J. W., and SCHENCK P. A. (1989d) The occurrence and identification of series of organic sulphur compounds in oils and sediment extracts II. Their presence in samples from hypersaline and non-hypersaline palaeoenvironments and possible application as source, palaeoenvironmental, and maturity indicators. *Geochim. Cosmochim. Acta* **53,** 1323–1341.

SINNINGHE DAMSTÉ J. S., EGLINTON T. I., RIJPSTRA W. I. C., and DE LEEUW J. W. (1990a) Characterization of sulfur-rich high molecular weight substances by flash pyrolysis and Raney Ni desulfurisation. In *Geochemistry of Sulfur in Fossil Fuels* (ed. W. L. ORR and C. M. WHITE); ACS Symp. Series 429, pp. 486–528. ACS.

SINNINGHE DAMSTÉ J. S., KOHNEN M. E. L., and DE LEEUW J. W. (1990b) Thiophene biomarkers for paleoenvironmental assessment and molecular stratigraphy. *Nature* **345,** 609–611.

TEGELAAR E. W., DE LEEUW J. W., DERENNE S., and LARGEAU C. (1989) A reappraisal of kerogen formation. *Geochim. Cosmochim. Acta* **53,** 3103–3106.

TISSOT B. P. and WELTE D. H. (1984) *Petroleum Formation and Occurrence,* 2nd ed. Springer-Verlag.

WINDIG W., KISTEMAKER P. G., and HAVERKAMP J. (1982) Chemical interpretation of differences in pyrolysis–mass spectra of simulated mixtures of biopolymers by factor analysis and graphical rotation. *J. Anal. Appl. Pyrol.* **3,** 199–212.